

# A bypass circuit for avoiding the hot spot in PV modules

Guerriero, Pierluigi; Tricoli, Pietro; Daliento, Santolo

DOI:

[10.1016/j.solener.2019.02.010](https://doi.org/10.1016/j.solener.2019.02.010)

License:

Creative Commons: Attribution-NonCommercial-NoDerivs (CC BY-NC-ND)

*Document Version*

Peer reviewed version

*Citation for published version (Harvard):*

Guerriero, P, Tricoli, P & Daliento, S 2019, 'A bypass circuit for avoiding the hot spot in PV modules', *Solar Energy*, vol. 181, pp. 430-438. <https://doi.org/10.1016/j.solener.2019.02.010>

[Link to publication on Research at Birmingham portal](#)

**Publisher Rights Statement:**

Checked for eligibility: 22/03/2019

**General rights**

Unless a licence is specified above, all rights (including copyright and moral rights) in this document are retained by the authors and/or the copyright holders. The express permission of the copyright holder must be obtained for any use of this material other than for purposes permitted by law.

- Users may freely distribute the URL that is used to identify this publication.
- Users may download and/or print one copy of the publication from the University of Birmingham research portal for the purpose of private study or non-commercial research.
- User may use extracts from the document in line with the concept of 'fair dealing' under the Copyright, Designs and Patents Act 1988 (?)
- Users may not further distribute the material nor use it for the purposes of commercial gain.

Where a licence is displayed above, please note the terms and conditions of the licence govern your use of this document.

When citing, please reference the published version.

**Take down policy**

While the University of Birmingham exercises care and attention in making items available there are rare occasions when an item has been uploaded in error or has been deemed to be commercially or otherwise sensitive.

If you believe that this is the case for this document, please contact [UBIRA@lists.bham.ac.uk](mailto:UBIRA@lists.bham.ac.uk) providing details and we will remove access to the work immediately and investigate.

# A Bypass Circuit for Avoiding the Hot Spot in PV Modules

Pierluigi Guerriero<sup>1</sup>, Pietro Tricoli<sup>2</sup>, Santolo Daliento<sup>1\*</sup>

<sup>1</sup> Department of Electrical Engineering and Information Technology, University of Naples Federico II,  
80125 Naples, Italy

<sup>2</sup> School of Electronic, Electrical and Systems Engineering, University of Birmingham  
Edgbaston, Birmingham, B15 2TT, UK

\*corresponding author: daliento@unina.it

## Abstract

The hot spot occurring in outlier solar cells is recognized as one of the main reliability issues for photovoltaic modules. Even though PV modules are qualified to sustain over-temperatures the hot spot can lead to accelerated aging and, sometimes, to unexpected failure; in severe cases, with the possible risk of fire. The standard countermeasure to contrast this phenomenon is the adoption of bypass diodes, whose role is to limit the maximum reverse voltage across outlier cells. However, since the current is not limited, power dissipation can be high. In this paper a bypass circuit, suited to completely avoiding the onset of the hot spot, is presented. The circuit is a substantial improvement of a previous version that was able to reduce power dissipation by reducing the voltage across the reverse biased solar cell. The improvement presented in this paper allow to completely cancel the current, thus avoiding power dissipation and, therefore, preventing the rising in temperature of the solar cell. The novelty with respect to comparable approaches is that the intervention of the circuit doesn't require the preliminary detection of the hot spot. Indeed, the circuit self-activates in the same operating conditions of standard diodes, without needing neither control logic nor power supply. Detailed circuit simulations and experiments are presented to evidence the capability of the circuit to fully prevent power dissipation, and consequent rising in temperature, in outlier cells.

*Keywords: hot spot, bypass diode, reliability, PV systems.*

## I. Introduction

In the last years the Photovoltaic (PV) technology experienced a huge increase of the installed capacity. In many countries the achievement of the fuel parity pushed large investments in the construction of new photovoltaic plants, as witnessed by the increment of tens of Gigawatt installed worldwide last year (Philipps and Warmuth, 2018). Among other factors, one of the key points which favored the success of this technology is its modularity, which makes the construction of utility scale power stations almost as easy as small scale domestic plants, with very reduced time to market. However, this strength is the major

38 weakness of the PV technology as well; in fact, the modularity means that thousands of elements  
39 (photovoltaic modules, which are in turn made of tens of series connected solar cells (Green, 1986)), are  
40 hardwired to build the desired power size. The consequence is that both fault location and fault fixing are  
41 extremely challenging and time-consuming issues. By taking in mind that the Return Of Investment  
42 (ROI), is not only dependent on the expected lifetime of the power plant, but also on the continuity of the  
43 power production, it is clear that plant shutdown for maintenance interventions should be avoided or, at  
44 least, minimized. It is quite obvious that the best strategy to prevent production losses, and consequent  
45 maintenance queries, is to improve the reliability of photovoltaic modules. In this regard, it is widely  
46 recognized that one of the main issues (Jordan and Kurtz, 2013; Kaplani, 2012; Sanchez-Friera et al.,  
47 2011) affecting the probability of faults in photovoltaic modules is the formation of hot spots (García et al.,  
48 2013), that is over-temperature typically localized on a portion of a solar cell. It should be remarked that  
49 the occurrence of hot spots is absolutely usual during normal operation of PV fields; indeed, the rising in  
50 temperature can be triggered by the simple presence of partial shading, even of very small area, like that  
51 caused by leaves or birth drops. In such conditions, in fact, solar cells get reverse biased, thus dissipating  
52 power and getting hot. In order to limit the maximum reverse bias, photovoltaic modules are equipped  
53 with bypass diodes that, as well explained in (Green, 1986), automatically turns on in presence of current  
54 mismatches. Unfortunately, bypass diodes cannot avoid the hot spot (Kim and Krein, 2015) occurrence.  
55 This fact means that photovoltaic modules should be manufactured to sustain over-temperatures without  
56 damages. In principle, the ability to sustain hot spots is certified for each model of commercially available  
57 photovoltaic module, by the qualification procedure dictated by the EN 61215 rules. This procedure  
58 verifies that the power dissipated by the hot spot cell, depending on the correct sizing of the bypass diode  
59 (“AN3432 ST Application note,” 2011), is low enough to avoid failures. However, it has been evidenced  
60 (Kim and Krein, 2015) that, due to the spread of solar cell parameters, damages can occur even though  
61 operating conditions are within expected safe limits. Moreover, it should be considered that recurring hot  
62 spot events can lead to accelerated ageing (Olalla et al., 2018), thus increasing the fault probability.

63 Above arguments lead to the conclusion that the over-temperature should be limited as much as possible.  
64 As mentioned above the main protecting strategy involves the adoption of bypass diodes. Indeed, as it is  
65 widely known, almost all crystalline photovoltaic modules are equipped with such diodes. Even though, as  
66 clarified in (Kim and Krein, 2015), they cannot avoid the hot spot, but just limit power dissipation, they  
67 have the fundamental feature to be fully compatible with the normal operation of photovoltaic modules,  
68 by automatically activating themselves only when, because of some current mismatch, the voltage  
69 supplied by the photovoltaic module reverses. Actually, whether or not the bypass diode, in case of  
70 mismatch, turns ON, is largely due the control algorithms for the Maximum Power Point Tracking

71 (MPPT). These algorithms can decide to lower the overall current delivered by the PV system, thus  
72 avoiding the turning ON of the bypass diode and the consequent reverse biasing of the outlier solar cell.  
73 Thus, a strategy which is encountering some success for limiting the hot spot, is based on the ability to  
74 recognize its occurrence so as to instruct the MPPT to keep the operating point of the system in a safe  
75 region (Spanoche et al., 2013). For example, in (Bressan et al., 2018) a shadow emulator based on FPGA  
76 is exploited to foresee the possible occurrence of hot spot. The limit of this approach is that it does not  
77 work for unexpected shadows coming from rubbish covering the cell; moreover, in such approaches, the  
78 power delivered by the whole system is dramatically reduced, because the current is limited to that  
79 supplied by the worst performing solar cell.

80 Different strategies presented so far involve improved bypass circuits able to reduce (or even suppress) the  
81 power dissipated in the reverse biased solar cell (D'Alessandro et al., 2014; Ghanbari, 2017; Niazi et al.,  
82 2018).

83 In this regard, it should be noted that power dissipation can be totally avoided by forcing the current to  
84 zero. Such a feature can be achieved by inserting a series switch for breaking the circuit when the  
85 conditions for the triggering of the hot spot are recognized, as for example proposed in (Dhimish et al.,  
86 2018). In such a case the key point is the reliable detection of unsafe operating conditions. In (Dhimish et  
87 al., 2018) thermal images were exploited to directly identify hot cells; after that, a series connected power  
88 MOSFET was driven in the OFF state. A more effective detection system was presented in (Kim et al.,  
89 2013), where the change of impedance of the monitored PV string is assumed as a sign of the presence of  
90 the hot spot. The detection required to periodically interrupt the MPPT to acquire the I-V curve of the  
91 string. When the hot spot is detected the current is interrupted by means of a series MOSFET. The  
92 drawback of this approach is that requires a microprocessor for each photovoltaic module; moreover, its  
93 effectiveness depends on the frequency of the I-V scan, in other words, the hot spot is not prevented, it is  
94 just suppressed some amount of time after its appearing.

95 In order to overcome the above drawback and with the aim to combine the benefits of the series switch  
96 with the self-activation of the standard bypass diode, a modified bypass circuit was presented in (Daliento  
97 et al., 2016). It exploited the decreasing voltage across the shaded photovoltaic module to drive in the  
98 pinch-off operating region a series connected MOSFET. As a result, the reverse voltage appearing across  
99 the shaded solar cell was diminished by the drain to source voltage of the MOSFET, thus transferring  
100 dissipated power from the solar cell to the power MOSFET. By adopting that circuit, the temperature of  
101 the hot cell decreased of some tens of Celsius degree; however, over-temperature was not completely  
102 avoided and the warming of the junction box (where the MOSFET was hosted) was a critical issue.

103 In this paper a substantial improvement of the circuit proposed in (Daliento et al., 2016) is presented.  
104 Differently from the previous solution, the new bypass circuit is able to completely suppress the current  
105 flowing into the reverse biased solar cell. Therefore, power dissipation cannot occur and the rising in  
106 temperature is fully prevented. As a result, the onset of the hot spot is totally avoided. Moreover, since the  
107 current is cancelled, the power MOSFET doesn't dissipate power and the warming of the junction box is  
108 prevented as well.

109 The new circuit still exploits the voltage across the photovoltaic module to drive the series connected  
110 power MOSFET, thus guaranteeing self-activation. The difference with respect to (Daliento et al., 2016) is  
111 a special designed driving circuit (see Fig.3), allowing the complete switching OFF of the series  
112 MOSFET. As will be shown in the following sections, the behavior of a photovoltaic module equipped  
113 with the proposed circuit is, from the terminals point of view, almost identical to that of a photovoltaic  
114 module equipped with a standard bypass diode.

115 The paper is organized as follows. Section II introduces the new circuit in comparison with the previous  
116 one. Section III provides a detailed description of the polarization and gives information about realization  
117 costs. Section IV describes actual operating modes achieved by means of circuit simulations. Section V  
118 reports experimental results. Finally, conclusions are drawn in Section VI.

119

## 120 **II. Bypass circuit operating principle**

121

122 As mentioned above the circuit proposed in this paper is an evolution of the circuit presented in (Daliento  
123 et al., 2016). In order to point out differences and new functionalities the previous circuit is shown in Fig.  
124 1b, while the additions proposed in this paper are shown in Fig. 2 and Fig. 3. Only the main features of this  
125 topology will be recalled here, more details can be found in (Daliento et al., 2016).

126

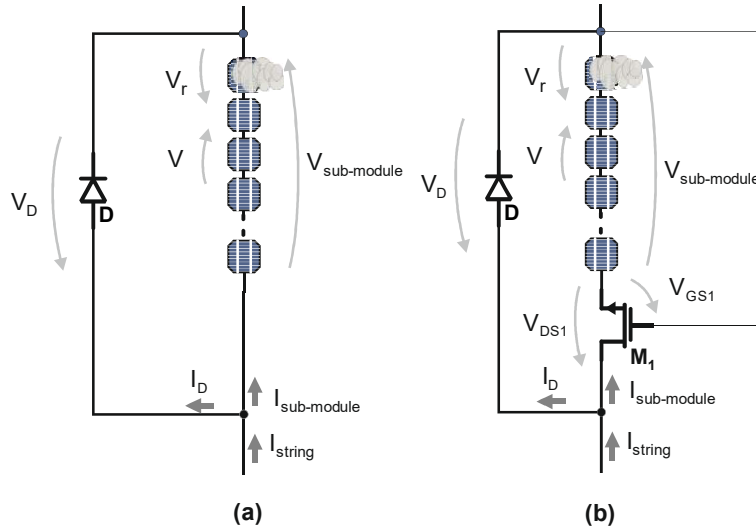


Fig. 1. Series of solar cells protected by standard bypass diode (a) and by an improved bypass circuit subtracting part of the reverse voltage from the shaded cell (b).

127  
128  
129  
130  
131

132 As can be seen, the figure shows both the standard arrangement (Fig. 1a), with a bypass diode "protecting"  
133 a group of  $N$  series connected solar cells (hereinafter referred to as sub-module), and the modified circuit  
134 (Fig. 1b), with the MOSFET  $M_1$  connected in series with the sub-module. The most important detail to  
135 note is that  $M_1$  is directly driven by the voltage,  $V_{\text{sub-module}}$ , supplied by the sub-module, which coincides  
136 with  $V_{\text{GS1}}$ . During normal operation (uniform irradiation and no limiting cells) this voltage is positive and  
137 quite high (about 10 V since the bypass diode is usually parallel connected to the series of about 20 solar  
138 cells). This voltage is high enough to push  $M_1$  in deep conduction where it exhibits a residual resistance of  
139 just few milliohms. In other terms, during uniform irradiation the presence of  $M_1$  is negligible and does  
140 not affect the behavior of the photovoltaic module. Conversely, when a solar cell limits the current  
141 supplied by the module (as an example because it is shadowed), the excess of current coming from the  
142 string deviates through the bypass diode, which limits to  $V_D$  the voltage at its terminal. Therefore, the  
143 reverse voltage across the limiting cell is

$$144 \quad V_r = (N-1)V + V_D, \quad (1)$$

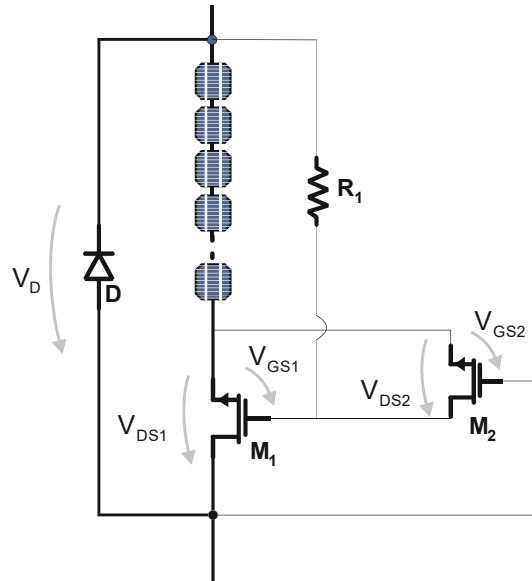
145 in the standard case of Fig. 1a, while it is

$$146 \quad V_r = (N-1)V + V_D - V_{\text{DS1}}, \quad (2)$$

147 in the presence of  $M_1$ .

148 In (2) (as shown in (Daliento et al., 2016))  $V_{\text{DS}}$  weakly depends on the current mismatch, being at least  
149 equal to the threshold voltage of  $M_1$ .

150 The drawback of the circuit of Fig. 1b is that  $M_1$  gets hot in place of the shaded cell.  
 151 In order to overcome this issue, the circuit shown in Fig. 2 could be adopted.  
 152 Two operating modes can be identified. The first corresponds to uniform behavior of all solar cells. In  
 153 such a case the circuit operation is identical to that of Fig. 1b. Indeed,  $M_1$  operates in deep conduction, so  
 154 that  $V_{DS1}$  is low. As can be seen,  $V_{DS1}$  is the driving voltage for  $M_2$  (coincides with the gate-source voltage  
 155 of  $M_2$ ), thus  $M_2$  is kept OFF and has no effects on the circuit. The second operating mode occurs in case of  
 156 current mismatch between  $I_{string}$  and  $I_{sub-module}$ . In such a case a positive feedback activates; indeed,  $V_{DS1}$   
 157 increases (as in the circuit of Fig. 1b) thus turning ON the MOSFET  $M_2$ , with the consequence that  $V_{DS2}$   
 158 decreases. Since  $V_{DS2}$  coincides with  $V_{GS1}$ ,  $M_1$  is driven in the OFF state and the current through the sub-  
 159 module is completely interrupted (while the string current,  $I_{string}$ , flows through the bypass diode).  
 160

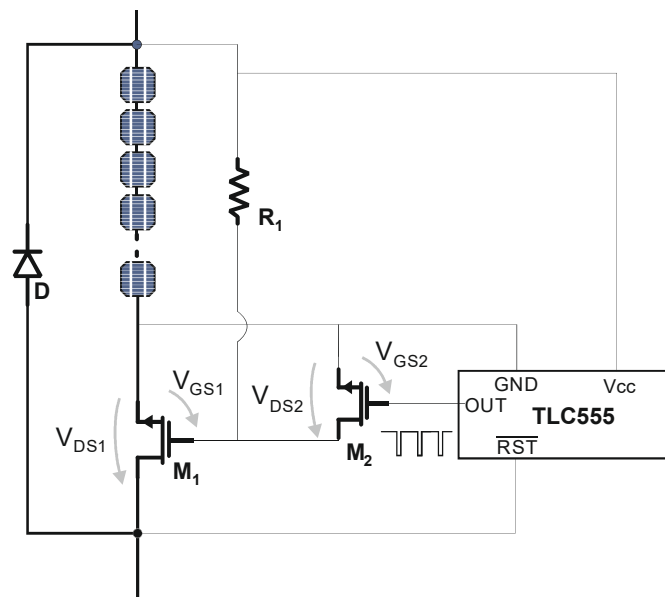


161  
 162 Fig. 2. Improved bypass circuit with a feedback MOSFET  $M_2$   
 163 to switch off the sub-module current.  
 164

165 Unfortunately, this very simple solution does not work well because the conduction of  $M_1$  can not be  
 166 recovered when the current mismatch ceases. In fact, once  $M_1$  has been interdicted, the rising of the  
 167 current is always prevented, even though the conditions for the bypass are removed.  
 168 Therefore, the circuit which is actually proposed in this paper is that of Fig. 3.  
 169 As can be seen, the feedback MOSFET  $M_2$  is now driven by the output voltage of a digital oscillator  
 170 TLC555. The oscillator is power supplied by  $V_{DS1}$ . Hence, as long as  $V_{DS1}$  is low (normal operation) the  
 171 oscillator is switched OFF, its output is low and  $M_2$  is OFF as well. When bypass conditions occur,  $V_{DS1}$   
 172 increases, the oscillator turns ON and starts to provide output signals alternatively high and low. As will

173 be shown in the next sections the duty cycle of the oscillator is chosen in such a way that the output signal  
 174 is kept high for about 97% of the time. During this interval of time  $M_2$  is ON and, as a consequence,  $M_1$  is  
 175 kept OFF. The lowering of the output signal of the oscillator can be seen as an attempt to turn ON  $M_1$ , if  
 176 bypass conditions are still present when the output of the oscillator returns to high  $V_{DS1}$  returns high as  
 177 well and, for another 97% of the time, the current cannot flow. Conversely, if bypass conditions are no  
 178 longer present, the attempt to turn ON  $M_1$  succeeds,  $V_{DS1}$  falls down, and the oscillator gets switched OFF,  
 179 thus returning in the normal operating conditions.

180



181

182

Fig. 3. New bypass circuit for the prevention of the hot spot.

183

184 The above solution fully prevents the rising in temperature of shaded cells. Moreover, differently from  
 185 other approaches, the circuit does not exploit microprocessors or other logic components. It is also  
 186 important to note that the circuit only consumes a negligible amount of power during bypass events, since  
 187 the TLC555 is sleeping for the rest of the time.

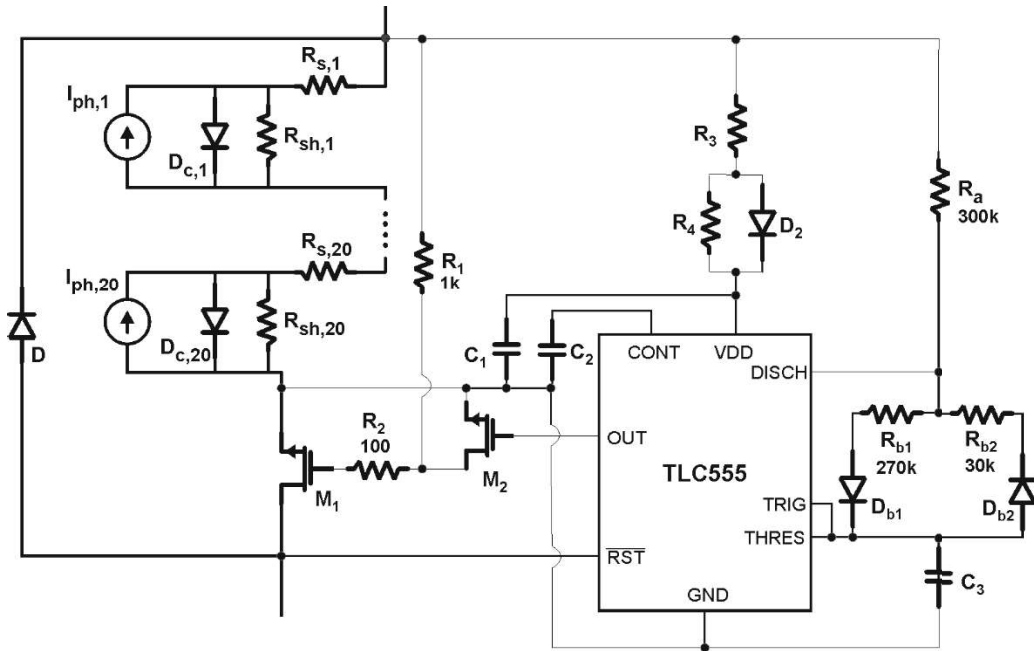
188 It is useful to note that the operation of the bypass circuit is strictly related to the architecture of the solar  
 189 module. The present form was designed for monocrystalline and polycrystalline solar modules, which are  
 190 made by groups (sub-modules) of series connected solar cells with accessible terminals. The proposed  
 191 circuit is not suitable for thin film technologies, because those solar panels are made by monolithically  
 192 integrated solar cells that do not give access to the internal terminals.



193 However, it is worth to point out that thin film solar panel based on multijunction solar cells can be  
 194 designed in such a way that each solar cell is provided with its own monolithically integrated bypass  
 195 diode. In this latter case the solar module is inherently safe and the hot spot is not a concern.

196 **III. Circuit realization and costs**

197  
 198 The complete bypass circuit, including all details about its continuous biasing, are reported in Fig.4



199  
 200 Fig. 4. Detailed circuit schematic of the proposed bypass solution.  
 201

202 As can be inferred, the figure is similar to Fig. 3, with the difference that the solar cells are described by  
 203 means of the one diode model (d'Alessandro et al., 2015);the TLC555 is shown along with its polarization  
 204 network, realized according with the guidelines reported in (Texas Instruments, 2016).In particular, the  
 205 group formed by  $R_3$ ,  $R_4$ ,  $C_1$ , and  $D_2$ , supplies the operating voltage to the integrated circuit. The capacitor  
 206  $C_1$ , which is connected from  $V_{DD}$  and ground (GND), stabilizes the supply voltage. At the start it is rapidly  
 207 charged through  $R_3$  and  $D_2$ . If the voltage supplied by the solar panel decreases, the discharge of  $C_1$  occurs  
 208 through the series  $R_4$ - $R_3$ , so that, choosing an high value for  $R_4$  (the values of all components are reported  
 209 in Table 1), guarantees slow discharge. It must be remarked that the TLC555 correctly operate with  
 210 polarization voltages between 2 V and 15 V, this fact means that the solar panel can supply the circuit in  
 211 all illumination conditions of practical interest. It is also important to point out that the circuit only leaks  
 212  $360 \mu A$  for its continuous operation, with a power consumption of few mW.

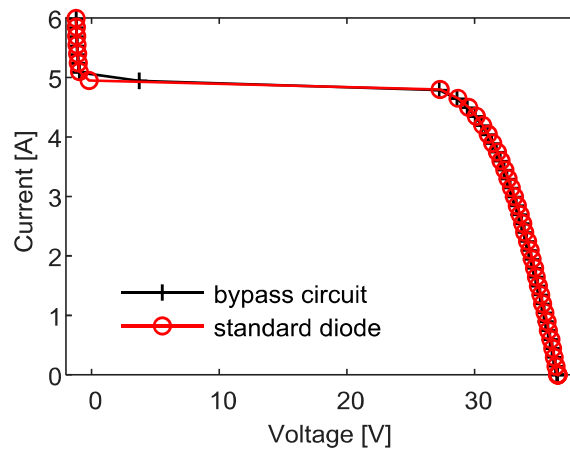
213 The group formed by  $R_a$ ,  $R_{b1}$ ,  $R_{b2}$ ,  $D_{b1}$ ,  $D_{b2}$ , and  $C_3$ , allows setting the frequency of the oscillator and the  
 214 duty cycle. Formulas for setting these parameters can be found in (Rogers, 2002). By summarizing we can

215 say that the resistances control the charging and discharging time constants of  $C_3$ , whose oscillating  
 216 voltage triggers oscillation period  $T$ , was chosen to have  $T=0.63$  s, while  $R_{b2}$ , related to the duty cycle,  
 217 was realized by means of a potentiometer allowing to vary the duty cycle in the range 2% - 50%.  
 218  $R_1$  is chosen to limit the current through  $M_2$  (when  $M_2$  is conducting) to few mA while  $R_2$  is chose to slow  
 219 down the switching time of  $M_1$ .  $C_2$  stabilizes the threshold for the triggering of the oscillations.  
 220 A photograph of the resulting prototype is shown in Fig. 5.  
 221



222  
 223 Fig. 5. Rear side photovoltaic module junction box containing  
 224 three bypass circuits. In the periphery the board contains  
 225 additional circuits for sensing purposes.  
 226

227 The I-V curve of the solar panel equipped with this prototype (see also Section V) are compared in Fig. 6  
 228 with the I-V curve of the same solar panel equipped with the standard bypass diode.



229  
 230 Fig. 6. I-V curves comparison: a 60-cells poly-Si module  
 231 equipped with standard diodes (red line) is compared to the  
 232 one adopting the proposed solution (black line).

233  
 234 As can be seen the two curves are almost identical; this means that the bypass circuit does not introduce  
 235 any disturbance when the solar panel is connected in a series string.  
 236 Some details about the cost of the circuit are reported in Table I. The extra cost with respect to the  
 237 standard bypass diode is about 2 €.

238 TABLE I

Part Name	Description	Unit Price [€]
TLC555	Astable Circuit	0.33 <sup>1</sup>
M <sub>1</sub>	N-channel MOFET 40V 100A	0.78 <sup>1</sup>
M <sub>2</sub>	N-channel MOFET 30V 2.6 A	0.21 <sup>1</sup>
D	Schottky diode 50V 20A	0.42 <sup>1</sup>
Biasing devices	SMD resistors ¼ W, Diodes, Ceramic capacitors	0.34
PCB	Production and Components Soldering	0.5
	Total cost	2.58

<sup>1</sup>online catalogue for a quantity of 1000 units.

239  
 240  
 241 The incidence of this cost depends on the number of solar cells forming the solar panel. Usually, one  
 242 bypass device protects about 20 solar cells so that the extra cost is about 0.1 € per solar cell. The incidence  
 243 of the cost in relation to the producible energy can be evaluated by assuming an expected lifetime for the  
 244 solar panel of 25 years and a average producible energy of 1300 kWh/kWp/year; for a 5 Wp solar cell this  
 245 means an extra cost of about 0.0001 €/ kWh. By considering that the cost of a solar cell is about 0.5 €/Wp,  
 246 the weight of the extra cost per kWh is about 1%.

247 Another concern for the bypass circuit is reliability. It is quite obvious that adding electronic devices  
 248 introduces reliability issues; however, in this case, the goal is to bring such issues outside the solar panel,  
 249 whose value is greater by orders of magnitude. Moreover, it should be considered that adopted power  
 250 devices are automotive devices rated to handle high currents (100 A) at high switching frequencies  
 251 (hundred of kHz) with an expected lifetime of several years. The proposed application is for much lower  
 252 currents and almost stationary operation, so that the expected lifetime becomes much longer than the  
 253 normal life cycle of the solar panel itself.

254  
 255 **IV. Circuit simulation**

256  
 257 Simulations were carried out by analyzing the circuit shown in Fig.4. This circuit represents a sub-module  
 258 made by 20 solar cells; simulations were carried out by connecting in series three of these circuits, thus  
 259 simulating the behavior of a photovoltaic module made by three sub-modules, hereinafter referred to as  
 260 #1, #2, and #3. In order to compare the proposed solution with the standard bypass approach, the

261 MOSFET  $M_1$  belonging to sub-module #1 was short circuited, thus reducing the circuit to that of Fig. 1a.  
262 A tracking algorithm, driving the operating point toward the maximum power point (MPP), was also  
263 embedded in the simulations.

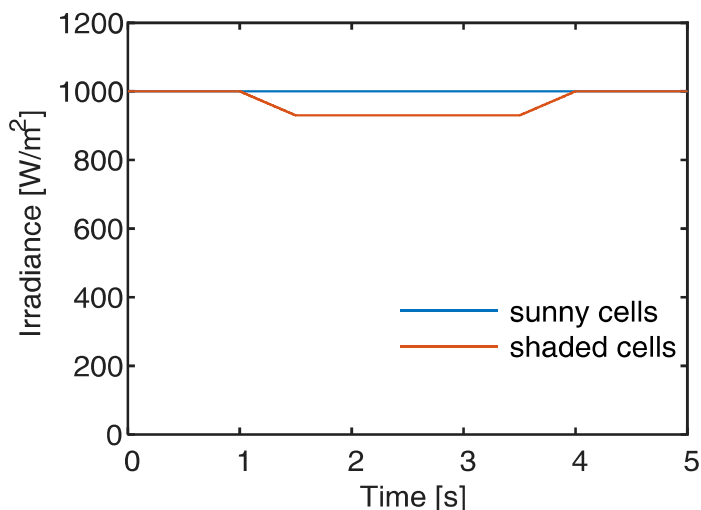
264 Simulated experiments were conducted by creating a current mismatch in sub-module #1 and sub-module  
265 #3 with respect to sub-module #2, so that the corresponding bypass devices turned ON. The mismatch was  
266 caused by assigning a reduced photogenerated current (current sources  $I_{ph,i}$  in Fig. 4) to only one solar cell  
267 per sub-module, so as to emulate the partial shadowing of sub-modules #1 and #3. As mentioned in the  
268 previous section such a situation leads to the reverse biasing of the shaded cells.

269 The current mismatch was chosen small enough to reproduce the worst conditions in terms of the power  
270 dissipated over the shaded cells, as defined by the EN 61215 and corresponding to a small shadow  
271 covering the cells. This situation has been also experimentally reproduced, as described in the next  
272 section.

273 The irradiance profile which is supposed to illuminate the solar cells is shown in Fig. 7.

274 As can be seen, sunny cells are supposed to be subject to a constant irradiance of  $1000 \text{ W/m}^2$  (i.e., 1 Sun),  
275 thus supplying their nominal current. In order to test the capability of the new bypass circuit to recognize  
276 the occurrence of the shadow, and to recover normal operation when this condition ceases, shaded cells  
277 were subject to a varying irradiance, passing from  $1000 \text{ W/m}^2$  to  $930 \text{ W/m}^2$  and vice-versa.

278 Let's start by analyzing the voltages across each sub-module, shown in Fig. 8.



279  
280  
281  
282

Fig. 7. Simulated irradiance profile adopted to emulate a current mismatch in the photovoltaic module.

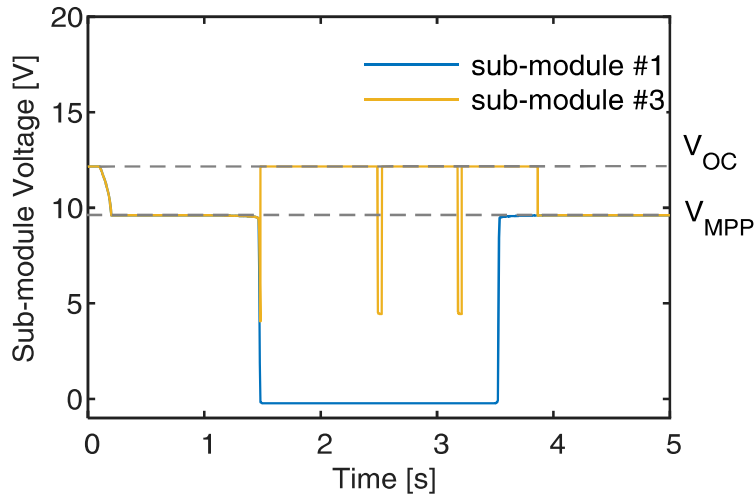


Fig. 8. Voltages supplied by the sub-modules during time varying irradiance conditions depicted in Fig.6.

283  
284  
285  
286

287 As starting condition,  $t=0$ , the sub-modules were assumed open circuited, as a consequence, the voltage at  
 288 their terminals was the open circuit voltage  $V_{oc}$ . Subsequently, the MPP Tracking (MPPT) algorithm  
 289 found the MPP and the voltage decreased to  $V_{MPP}$ . At  $t=1s$  (see Fig. 7) the irradiance over shaded cells  
 290 started to decrease and, at about  $t=1.5s$ , the current mismatch was large enough to trigger the turn ON of  
 291 the protection devices. It is important to note that both protection systems turn ON simultaneously, thus  
 292 evidencing that no delays are introduced by the new circuit. On the other hand, the behavior of the two  
 293 sub-modules is totally different. In fact, while the voltage across sub-module #1 was small and negative  
 294 (equal to the voltage drop across the forward biased bypass diode), the voltage across sub-module #3  
 295 reached  $V_{oc}$ , thus demonstrating that the series MOSFET interrupted the current. As can be seen, the  
 296 voltage across sub-module #3 decreased periodically, this fact is due to the action of the oscillator that  
 297 checks the persistence of the bypass conditions, as long as a current mismatch exists the voltage returns to  
 298  $V_{oc}$ ; conversely, when the mismatch ceases, sub-module #1 promptly recovers  $V_{MPP}$ , while sub-module  
 299 #3 waits for the change of state of the oscillator, after that,  $V_{MPP}$  is recovered as well. Therefore, the  
 300 maximum time allowed for the temperature of the shaded cell to increase is equal to the period of the  
 301 oscillator.

302 The effect of the bypass circuits on the shaded cells is better evidenced in Fig. 9.

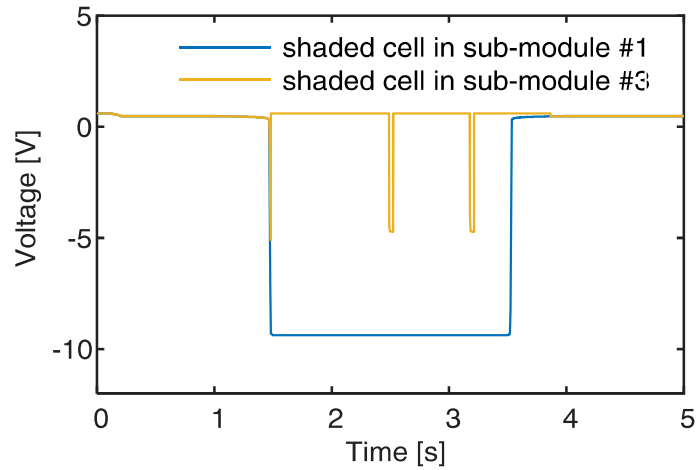


Fig. 9. Voltages across shaded solar cells in sub-modules protected by a standard bypass diode (blue curve) and by the proposed bypass circuit (yellow curve).

303  
 304  
 305  
 306  
 307  
 308 As can be seen, during the mismatch, the shaded cell in sub-module #1 was strongly reverse biased (thus  
 309 heating up), while the shaded cell in sub-module #3 was open circuited for the most part of the time. It is  
 310 interesting to note that the reverse voltage across the shaded cell in sub-module #3 remains lower than the  
 311 other also during the shadow checks; this fact depends on the presence of the series MOSFET which  
 312 shares part of the total voltage, as illustrated in Fig. 1.  
 313 Finally, Fig. 10a shows the drain to source voltages,  $V_{DS}$ , across the MOSFETs  $M_1$  and  $M_2$  of the bypass  
 314 circuit, that, according to Fig. 3 coincide, respectively, with the supply voltage of the oscillator and with  
 315 the driving voltage,  $V_{GS1}$ , of  $M_1$ ; while, Fig. 10b reports the output voltage of the oscillator, that coincides  
 316 the driving voltage of  $M_2$ .

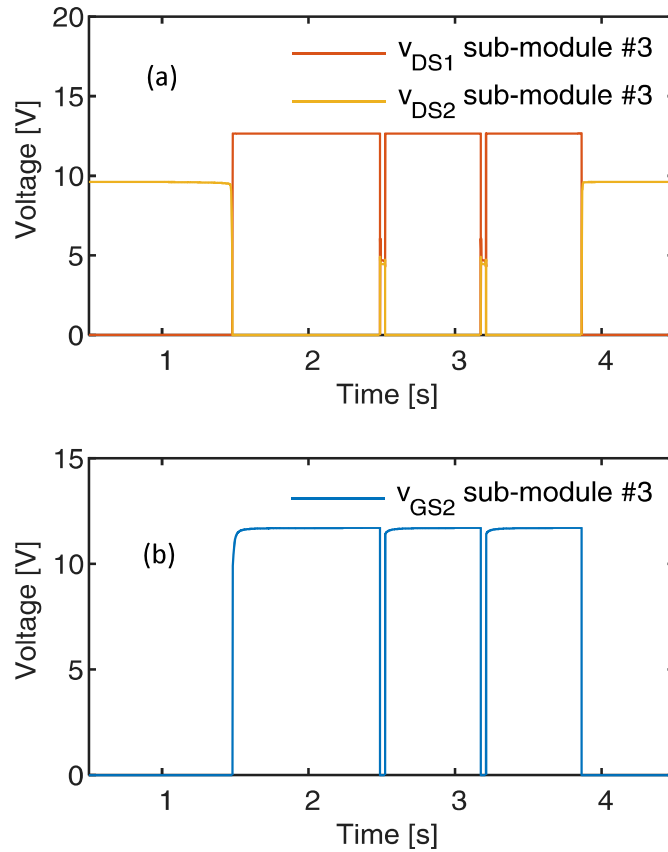


Fig. 10. Driving voltages of the active devices forming the proposed bypass circuit.

317  
 318  
 319  
 320  
 321 During normal operation (no current mismatch), the driving voltage for  $M_1$  ( $V_{DS2}$ ) is high (equal to  $V_{MPP}$ )  
 322 and  $V_{DS1}$  is near zero; when the mismatch occurs ( $t=1.5$ s), the oscillator is switched ON and its output  
 323 signal ( $V_{GS2}$  in Fig. 10b) starts to oscillate. When  $V_{GS2}$  is high,  $M_2$  is turned ON, as evidenced by  $V_{DS2}$  in  
 324 Fig. 9a that decreases to near zero, consequently  $M_1$  is switched OFF. When  $V_{GS2}$  is low (mismatch check)  
 325  $M_1$  turns ON, but, if the mismatch is still present,  $V_{DS1}$  remains high enough to power supply the  
 326 oscillator, so that  $M_1$  turns OFF again when  $V_{GS2}$  recovers the high value. On the contrary, when the  
 327 attempt to turn ON  $M_1$  ( $V_{GS2}$  low) occurs in absence of current mismatch,  $V_{DS1}$  decreases to near zero, so  
 328 that the oscillator is switched OFF and the normal operation is recovered.

329  
 330 **V. Experiments**  
 331

332 In order to experimentally verify the performance of the new bypass circuit an electronic board (shown in  
 333 Fig.5), suitable to be hosted in the standard junction box mounted in the rear side of photovoltaic modules,  
 334 was designed and fabricated.

335 The photovoltaic module adopted for the experiments is shown in Fig. 11; it was made by 60 solar cells,  
336 grouped in three sub-modules (hereinafter referred to as #1, #2, and #3 as for the simulations), the board  
337 contained three separate bypass circuits. In order to test the new circuit in comparison with the standard  
338 bypass diode the MOSFET  $M_1$  of the bypass circuit of sub-module #1 was short circuited as in the  
339 simulations. Two kinds of experiments were carried out, in the first case a dynamic shadow, advancing  
340 and regressing over a solar cell embedded in sub-module #3 was considered. In such a case, the capability  
341 of the bypass circuit to recognize the mismatch and to recover the normal operation, was tested. This  
342 experiment can be directly compared with the simulations. In the second case, in order to test the  
343 capability of the circuit to prevent the hot spot, two solar cells, belonging, respectively, to sub-module #1  
344 and sub-module #3, were partially obscured.  
345



346  
347 Fig. 11. The 60-cells module adopted for experiments.  
348 Second case test set-up: partially shaded solar cells belonging  
349 to different sub-modules. The cell on the left is protected by  
350 the standard bypass diode, the cell on the right by the new  
351 bypass circuit.  
352

353 In the first case significant electrical parameters were monitored. A photograph of the signals acquired by  
354 a digital oscilloscope is shown in Fig. 12.





Fig. 12. Digital oscilloscope view of electrical signals during a bypass event.

355

356

357

358 The yellow and the blue curves are, respectively, the string current and the current in sub-module #3. The  
 359 purple and the green curves are, respectively, the drain to source voltage of  $M_1$  and the gate to source  
 360 voltage of  $M_1$ .

361 To make the interpretation easier, signals are shown separately in the following figures. From these  
 362 figures it can be derived that the period of the oscillator was set to about 0.6s with duty cycle 96.5%;  
 363 hence, the duration of the mismatch check was about 21ms.

364 As can be inferred from Fig. 13a, sub-module #3 was shadowed at about -1.5 s.

365 The correct intervention of the bypass circuit is witnessed by the interruption of the sub-module current, as  
 366 well as by  $V_{DS1}$ , reported in Fig. 13b, that reached the open circuit voltage. Moreover, the figure shows  
 367 that the driving voltage of  $M_1$ ,  $V_{GS1}$ , periodically tried to turn ON  $M_1$ , but, since shadow was not yet  
 368 removed, the open circuit condition was promptly recovered when  $V_{GS1}$  returned low.

369 The return to normal operation, when the shadow was removed, is shown in Fig. 14 (note that a new  
 370 timescale is adopted because the figure comes from a new acquisition).

371 In this case, in the interval of time between 0.5 s and 1s the shadow was removed, so that, after the first  
 372 time  $V_{GS1}$  was made high, at about 1s,  $M_1$  turned ON ( $V_{DS1}$  went to zero) and the sub-module supplied  
 373 again the normal operating current.

374 The definitive evidence of the correct behavior of the bypass circuit is given by the thermal analysis. The  
 375 experiment was carried out by applying an opaque shield on two solar cells, as shown in the photograph  
 376 reported in Fig. 11.

377

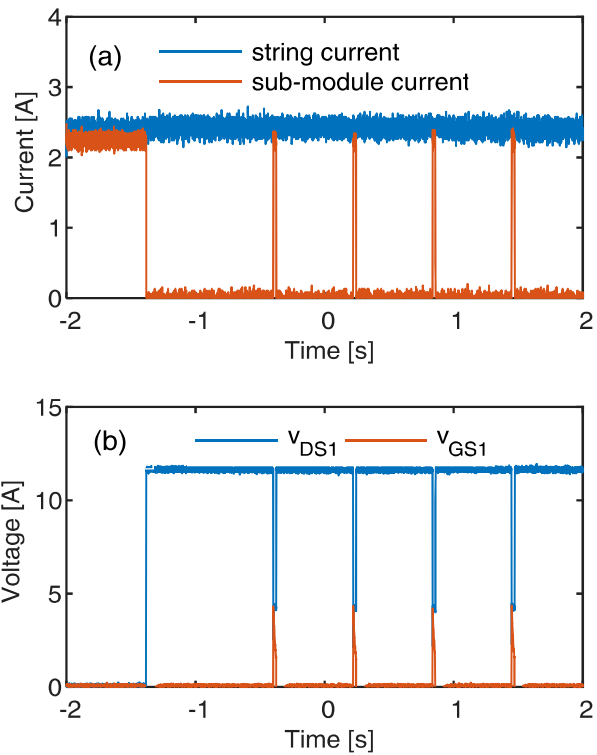


Fig. 13. (a) Currents and (b) voltages measured at the onset of the bypass event.

378  
379  
380

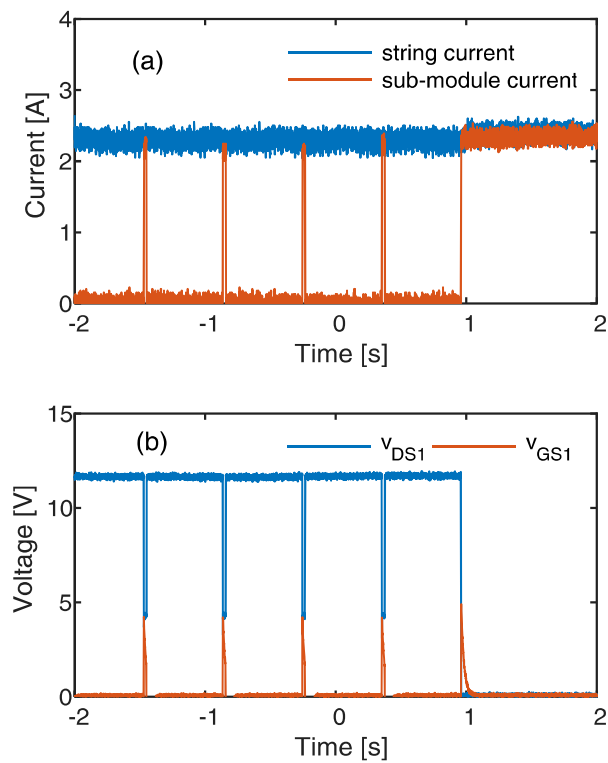


Fig. 14. (a) Currents and (b) voltages measured at the end of the bypass event.

381  
382

383 The area of the shields was chosen by following the procedure for the "Hot spot endurance test" described  
 384 in the EN 61215 to cause the maximum expected power dissipation over the solar cells. The shaded cell  
 385 in the left side belonged to sub-module #1, hence it was protected by the standard bypass diode only; the  
 386 shaded cell in the right side belonged to sub-module #3, hence it was protected by the modified bypass  
 387 circuit. During this experiment the irradiance was about  $800 \text{ W/m}^2$ , corresponding to a photogenerated  
 388 current supplied by the sunny cells of about 6.7 A.

389  
 390 Current and voltages corresponding to such conditions are reported in Fig. 15.

391 In particular, in Fig. 15a the current supplied by the sunny cells, indicated as "string current", is compared  
 392 to the currents flowing through the shaded cells. As can be seen, the current flowing through the cell not  
 393 protected by the bypass circuit is about 5.85 A, coinciding with the current at the maximum power point  
 394 MPP (according to the operating conditions prescribed by the EN 61215). The current flowing through the  
 395 cell protected by the bypass circuit is zero, thanks to the opening of the series MOSFET. At the same time,  
 396 as shown in Fig. 15b, the voltage across the sub-module with the bypass circuit was about 11 V, which is  
 397 the open circuit voltage (since no current is flowing), while the voltage across the sub-module without the  
 398 bypass circuit is -0.43 V (because of the intervention of the standard bypass diode). Consequently, the  
 399 power dissipated by the sub-module equipped with the bypass circuit (Fig. 15c) was zero, while the sub-  
 400 module not protected by the bypass circuit was dissipating an overall power P of about 2.5 W.

401 In this regard it is worth noting that, actually, only the shaded solar cell was dissipating power, while the  
 402 others were working at the MPP. Therefore, the power dissipated by the shaded solar cell can be evaluated  
 403 by considering that the overall power P produced by the sub-module is given by

$$404 \quad P = \sum_{i=1}^{20} V_i \cdot I_{string} = 19 \cdot V_{MPP} \cdot I_{string} + V_{Shad} \cdot I_{string} \quad (3)$$

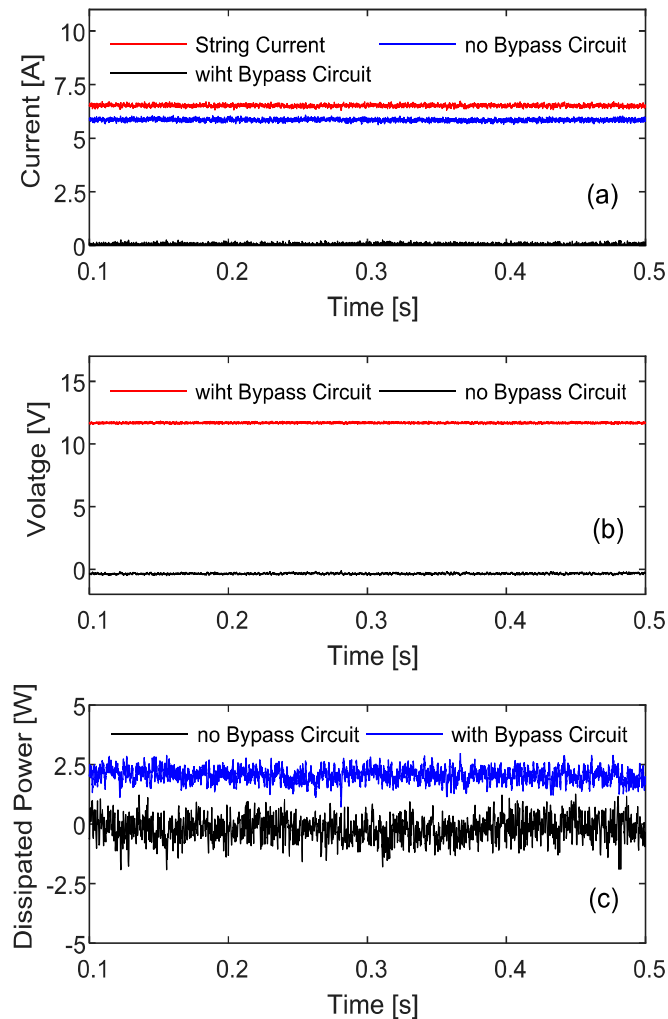
405 where  $V_{shad}$  is the voltage across the shaded cell. This equation leads to

$$406 \quad V_{Shad} \cdot I_{string} = P - 19 \cdot V_{MPP} \cdot I_{string} = -55.8W \quad (4)$$

407 In contrast, the shaded cell protected by the bypass circuit dissipated zero power.

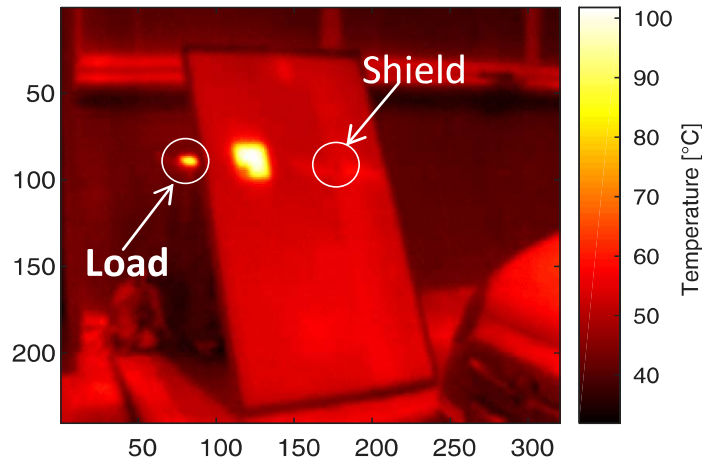
408 Above results justify the thermal image shown in Fig. 16, taken by means of an IR camera FLUKE TiS56.  
 409 As can be seen, the solar cell on the left side, not protected by the bypass circuit, got extremely hot, while  
 410 the solar cell protected by the bypass circuit was cold (the position of the shield can be individuated as a  
 411 colder area in the white circle). It is interesting to note that the right side of the photovoltaic module (that  
 412 coincides with sub-module #3) showed an average temperature higher than the left side, this is a further  
 413 evidence that sub-module #3 operated in open circuit conditions (it is worth remembering that open  
 414 circuited solar cells do not convert Sun power into electrical power, hence, the operating temperature gets  
 415 higher). The hot shape on the left, off the photovoltaic module, is the load adopted to fix the operating

416 point.



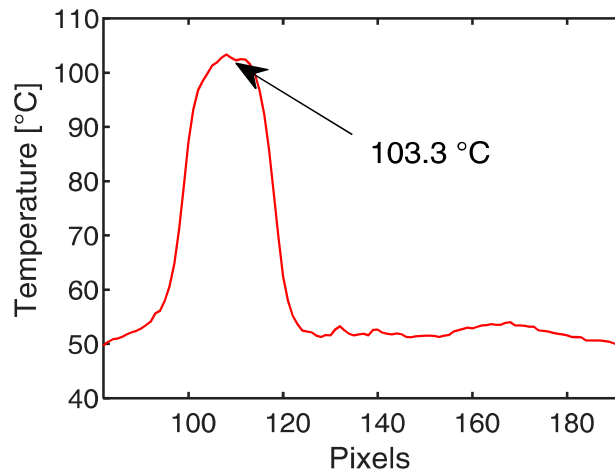
417  
418 Fig. 15. Currents (a), and voltages (b) corresponding to the  
419 shading conditions of Fig. 11. Power dissipation (c) with and  
420 without the bypass circuit.  
421

422 From this figure the temperature profile along a cutting line passing through the center of the two shaded  
423 cells has been extracted. This profile, reported in Fig. 17, shows that the hot cell reached a temperature of  
424 about 103°C, with a temperature increment of about 50°C with respect to normal operating cells.  
425 Conversely, the shaded cell, belonging to sub-module #3 and protected by the new bypass circuit,  
426 remained at the normal operating temperature, with an expected small increment on the exposed surface  
427 depending on the open-circuit operation.



428  
429  
430  
431

Fig. 16. Thermal image of the partially shaded photovoltaic module shown in Fig.13.



432  
433  
434  
435

Fig. 17. Thermal profile along a cutting line passing through the center of the shaded solar cells.

## VI. Conclusions

436  
437  
438  
439  
440  
441  
442  
443  
444

In this paper a new bypass circuit has been presented. The circuit prevents the formation of hot spots in malfunctioning solar cells by interrupting the current circulating in the corresponding sub-module, thus inhibiting power dissipation. With respect to other solutions based on the same principle, the proposed circuit has an "analogical" behavior, in the sense that it is self-activating when mismatch conditions occur, without needing micro-processors or other complex logic circuits. Simulations and experiments have evidenced that the hot spot can be effectively prevented. In the worst case operating conditions, as defined by the EN 61215, a difference of about 50 °C, has been found between a shaded solar cell protected by a

445 standard bypass diode and, in the same operating conditions, a solar cell protected by the new bypass  
446 circuit.

447

#### 448 **References**

449 AN3432 ST Application note [WWW Document], 2011. <https://doi.org/019041> Rev 1

450 Bressan, M., Gutierrez, A., Garcia Gutierrez, L., Alonso, C., 2018. Development of a real-time hot-spot  
451 prevention using an emulator of partially shaded PV systems. *Renew. Energy* 127, 334–343.  
452 <https://doi.org/10.1016/j.renene.2018.04.045>

453 d'Alessandro, V., Di Napoli, F., Guerriero, P., Daliento, S., 2015. An automated high-granularity tool for  
454 a fast evaluation of the yield of PV plants accounting for shading effects. *Renew. Energy* 83, 294–  
455 304.

456 d'Alessandro, V., Guerriero, P., Daliento, S., 2014. A simple bipolar transistor-based bypass approach for  
457 photovoltaic modules. *IEEE J. Photovoltaics* 4, 505–513.

458 Daliento, S., Di Napoli, F., Guerriero, P., d'Alessandro, V., 2016. A modified bypass circuit for improved  
459 hot spot reliability of solar panels subject to partial shading. *Sol. Energy* 134.  
460 <https://doi.org/10.1016/j.solener.2016.05.001>

461 Dhimish, M., Holmes, V., Mather, P., Sibley, M., 2018. Novel hot spot mitigation technique to enhance  
462 photovoltaic solar panels output power performance. *Sol. Energy Mater. Sol. Cells* 179, 72–79.  
463 <https://doi.org/10.1016/j.solmat.2018.02.019>

464 García, M., Marroyo, L., Lorenzo, E., Marcos, J., Pérez, M., 2013. Observed degradation in photovoltaic  
465 plants affected by hot-spots. *Prog. Photovoltaics Res. Appl.* 24, 1292–1301.  
466 <https://doi.org/10.1002/pip.2393>

467 Ghanbari, T., 2017. Hot spot detection and prevention using a simple method in photovoltaic panels. *IET*  
468 *Gener. Transm. Distrib.* 11, 883–890. <https://doi.org/10.1049/iet-gtd.2016.0794>

469 Green, M.A., 1986. *Solar cells : operating principles, technology and system applications*. University of  
470 New South Wales., Kensington.

471 Jordan, D.C., Kurtz, S.R., 2013. Photovoltaic Degradation Rates-an Analytical Review. *Prog.*  
472 *Photovoltaics Res. Appl.* 21, 12–29. <https://doi.org/10.1002/pip.1182>

473 Kaplani, E., 2012. Detection of degradation effects in field-aged c-Si solar cells through IR thermography  
474 and digital image processing. *Int. J. Photoenergy* 2012. <https://doi.org/10.1155/2012/396792>

475 Kim, K.A., Krein, P.T., 2015. Reexamination of Photovoltaic Hot Spotting to Show Inadequacy of the  
476 Bypass Diode. *IEEE J. Photovoltaics* 5, 1435–1441.  
477 <https://doi.org/10.1109/JPHOTOV.2015.2444091>

478 Kim, K.A., Krein, P.T., Seo, G.S., Cho, B.H., 2013. Photovoltaic AC parameter characterization for  
479 dynamic partial shading and hot spot detection. *Conf. Proc. - IEEE Appl. Power Electron. Conf.*  
480 *Expo. - APEC* 2, 109–115. <https://doi.org/10.1109/APEC.2013.6520194>

481 Niazi, K., Khan, H.A., Amir, F., 2018. Hot-spot reduction and shade loss minimization in crystalline-  
482 silicon solar panels. *J. Renew. Sustain. Energy* 10, 033506. <https://doi.org/10.1063/1.5020203>

483 Olalla, C., Hasan, M., Deline, C., Maksimović, D., 2018. Mitigation of Hot-Spots in Photovoltaic Systems

484 Using Distributed Power Electronics. *Energies* 11, 726. <https://doi.org/10.3390/en11040726>

485 Philipps, S., Warmuth, W., 2018. PHOTOVOLTAICS REPORT [WWW Document].

486 Rogers, P., 2002. Design low-duty-cycle timer circuits [WWW Document]. Bill Travis. URL  
487 [www.edn.com](http://www.edn.com)

488 Sanchez-Friera, P., Piliouline, M., Pelaez, J., Carretero, J., Cardona, M.S. de, 2011. Analysis of  
489 degradation mechanisms of crystalline silicon PV modules after 12 years of operation in Southern  
490 Europe. *Prog. PHOTOVOLTAICS Res. Appl.* 19, 658–666. <https://doi.org/10.1002/pip.1083>

491 Spanoche, S.A., Stewart, J.D., Hawley, S.L., Opris, I.E., 2013. Model-Based Method for Partially Shaded  
492 PV Module Hot-Spot Suppression. *IEEE J. Photovoltaics* 3, 785–790.  
493 <https://doi.org/10.1109/JPHOTOV.2012.2230054>

494 Texas Instruments, 2016. TLC555 LinCMOS Timer [WWW Document]. URL  
495 <http://www.ti.com/lit/ds/symlink/tlc555.pdf>

496